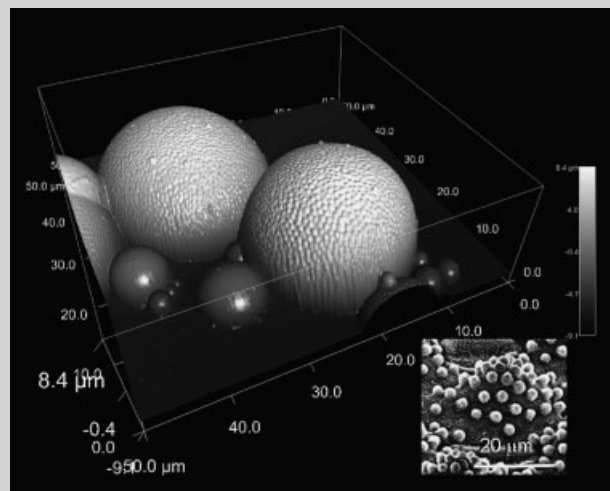


Summary: We describe a way to obtain biomimetic, hierarchical surface morphologies. In order to mimic natural surfaces more accurately such as lotus leaves and gecko feet, we employ a strategy that bears many of the attractive characteristics of natural materials synthesis. The system in question consists of a photocurable monomer and water. To this quasi-two-component system we add polymer latex spheres. The monomer–water interface is then manipulated according to the well-established science of complex fluids. Drawing from the rich phase behavior of particle-stabilized emulsions, we demonstrate the creation of complex biomimetic morphologies over many length scales. The resulting structures are then solidified by crosslinking the monomer with UV light.



Comparison of an AFM image of a PMMA colloidosome assembly with that of the textured surface of a superhydrophobic *Hygoryza aristata* leaf (inset).

Generation of Hierarchical Topologies from Photocrosslinkable, Particle-Stabilized Emulsions^a

Jason J. Benkoski,* Hua Hu, Alamgir Karim

National Institute of Standards and Technology, Gaithersburg, Maryland 20899, USA

E-mail: jason.benkoski@nist.gov

Received: April 19, 2006; Revised: June 1, 2006; Accepted: June 6, 2006; DOI: 10.1002/marc.200600272

Keywords: biomimetic; colloids; crosslinking; interfaces; microstructure; photopolymerization; self-assembly

Introduction

Surface properties often play a central role in the design of advanced materials for demanding applications. Although the design goals may often be met through surface chemistry, recent discoveries suggest that greater gains may be made through control of topology. Nowhere can this better be seen than in nature. The microscopic structure of shark skin has been shown to play a critical role in reducing frictional drag.^[1,2] One may also look to the iridescent patterns on butterfly wings, which result not from pigmentation, but from the interference and diffraction of light from the nanostructured ridges on their surfaces.^[3]

As seen above, different length scales are optimal for different applications. In many cases the size scale is set by tradeoffs between competing properties. When tradeoffs occur, nature overcomes this limitation by creating a hierarchy of surface structures over multiple length scales. Such hierarchically rough surfaces are responsible for both the superhydrophobicity of lotus leaves^[4–7] and the unmatched adhesive properties of gecko feet.^[8–10] When properly applied, this strategy makes it possible to optimize the desired properties while minimizing any unwanted side effects.

The main lesson to be learnt from nature is that extraordinary properties can be achieved with ordinary materials. Observe that none of the starting materials are particularly exotic (e.g., keratin, wax, chitin). Instead, we see that the choice of material appears to depend less on properties than on availability. In this respect, nature makes a strong case for

^a Official contribution of the National Institute of Standards and Technology; not subject to copyright in the United States.

focusing on advanced processing rather than advanced chemistry. We, therefore, present a platform that can create a hierarchy of well-defined surface features at multiple length scales.

In order to match nature's control over topology, we will employ a system that bears many of the attractive features of natural materials synthesis: an aqueous environment, minimal waste, low energy, and low cost. The system in question will consist of a photopolymerizable monomer and water. Since the two liquids essentially form an oil–water interface, the topology of the oil phase can be easily manipulated using surface-active lipids or particles. By drawing from the rich phase behavior of complex fluids, it will be possible to create intricate morphologies from colloidal length scales down to molecular dimensions.^[11] In this communication, we focus on the use of particulate additives for controlling the topology.

Colloidal particles have already been successfully used to generate topologically complex surfaces. Using layer-by-layer deposition of polyelectrolytes and charged nanoparticles, several groups have fabricated stable organic–inorganic hybrid films with controlled roughness on both micron and nanometer length scales.^[12–14] Such structures exhibited either excellent superhydrophobicity or superhydrophilicity depending on the particle type. Particle-stabilized emulsions are another example of synthetic structures possessing hierarchical structure. In a manner similar to that described above, Angelatos et al. have described the creation of nanoparticle capsules by infiltrating gold nanoparticles into the shell of polyelectrolyte multilayer capsules.^[15] With respect to the current study, our approach builds upon previous work in which nanoparticle-coated surfaces were formed by creating particle-stabilized emulsions.^[16–20] Although the fabrication of robust nanoparticle colloidosomes has been achieved by direct particle binding or gelation of the aqueous phase,^[21–24] the current platform is unique in that it performs irreversible fixation through the oil phase. The platform is also unique for the fact that the colloidosomes, once crosslinked, can be used to stabilize even larger emulsion droplets and form the basis for “supracolloidosomes,” thus building up many generations of hierarchical topology.

Experimental Part

Samples were prepared in the configuration shown in Figure 1. It is a quasi-two component system made up of an oil and a water phase. The oil phase consisted of 1,12-dodecane-diol-dimethacrylate (DDMA) and 2% by mass fraction Irgacure 819 (bis(2,4,6-trimethylbenzoyl)-phenylphosphineoxide, Ciba Specialty Chemicals^a). Irgacure 819 is a particularly efficient

^a Certain commercial equipment, instruments, or materials are identified in this paper in order to specify the experimental procedure adequately. Such identification is not intended to imply recommendation or endorsement by the National Institute of Standards and Technology, nor is it intended to imply that the materials or equipment identified are necessarily the best available for the purpose.

photoinitiator, which is designed for the radical polymerization of acrylate monomers upon UV light exposure. When exposed to a 365 nm high pressure mercury lamp at an intensity of $8 \text{ mW} \cdot \text{cm}^{-2}$, solidification of the resin was achieved within 1 to 5 s. The aqueous phase was buffered using $10 \text{ mmol} \cdot \text{L}^{-1}$ *N*-(2-hydroxyethyl)piperazine-*N'*-2-ethanesulfonic acid (HEPES), $100 \text{ mmol} \cdot \text{L}^{-1}$ NaCl, and it was adjusted to a pH of 8.

With respect to the self-assembly process, it was carried out at room temperature by first dispersing uncharged, crosslinked 390 nm poly(methyl methacrylate) (PMMA) latex spheres within 0.1 mL of DDMA. After adding the oil suspension to 4 mL of buffer, the system was vortexed in a glass vial until a uniform suspension of colloidosomes were formed. The suspension was then exposed to the UV source for 5 min. To the solidified colloidosome suspension was added an additional 0.5 mL of liquified DDMA. The system was not shaken in this case to allow the DDMA to form a continuous film across the top of the aqueous suspension. Five min were then allowed for colloidosomes to segregate to the liquid–liquid interface, and afterwards the system was exposed to the UV source a second time.

Also tested were dilute dispersions of the 390 nm PMMA particles at a planar oil–water interface (no vortexing). These experiments were performed to study only the interactions between the particles themselves. The 390 nm PMMA particles were dispersed in a continuous gradient from 5 vol.-% by bulk to 0%. After 15 min at room temperature, the DDMA was crosslinked to obtain a snapshot of the resulting particle configurations. Images were then taken at several locations to see whether aggregation occurred above a critical areal density. The majority of micrographs were obtained using either a Digital Instruments^a 3100 atomic force microscope (AFM) or an Asylum Research^a MPF-3D AFM. Larger particulate assemblies were inspected using a Nikon^a Optiphot-2 light optical microscope (LOM).

Results and Discussion

As seen in Figure 2, dilute dispersions of the PMMA particles at the planar DDMA–water interface (no vortexing) exhibited no agglomeration. Even at a 25% area fraction, the placement of particles still appeared to be random. Only when the interface was saturated did the particles exhibit random close packing. An example of such packing can be seen in Figure 3, which shows a small grouping of colloidosomes formed from an emulsion of DDMA that was stabilized with 390 nm PMMA particles. The inset shows the surface topology of a superhydrophobic lotus leaf for comparison.^[4] Figure 4 displays a light optical micrograph of the colloidosome assemblies at low magnification. At the largest size scale the organization is characterized by the polydispersity of the colloidosomes and the irregularity of their aggregates. Lower polydispersity was attainable, and it could be achieved by increasing the vortexing time during the second step of processing (Figure 1).

Figure 3 hints at intriguing possibilities for the generation of hierarchical organization. In addition to technological

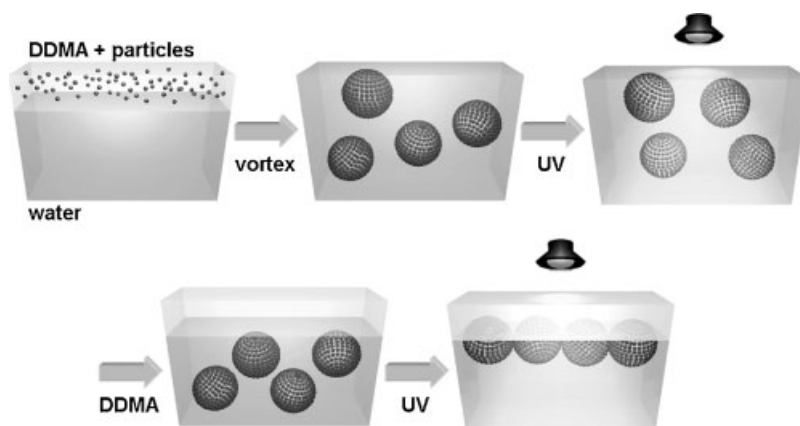


Figure 1. Schematic display of sample preparation. The first step is to add 0.1 mL of DDMA containing 5 vol.-% of 390 nm PMMA particles to 4 mL of buffer. Next, the mixture is vortexed until particle-coated oil droplets are formed. The droplets are then illuminated with UV light. Once the colloidosomes are fully crosslinked, a fresh layer of DDMA is added to the top of the buffer, and the colloidosomes are allowed to partition to the DDMA–water interface. Finally, the system is exposed to UV light a second time to crosslink the newly added oil layer.

applications such as self-cleaning surfaces, the current platform can serve as a model system for understanding the fundamental physics behind the formation of hierarchical topologies. We begin with the situation depicted in Figure 2, where the 390 nm PMMA particles interact via simple hard-core repulsion and no apparent long range electrostatic interactions. The van der Waals interaction energy^[25] (E_{vdW}) for two particles is given by

$$E_{vdW} = -AR/12D \quad (1)$$

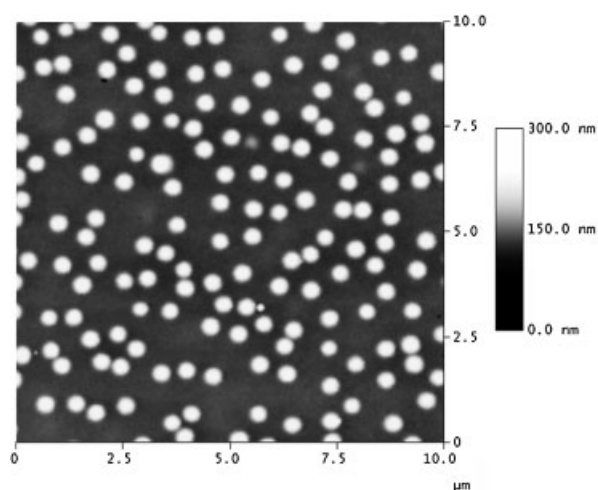


Figure 2. Representative AFM micrographs of 390 nm PMMA spheres taken after 15 min for a buffer consisting of 10 mmol · L⁻¹ HEPES, 100 mmol · L⁻¹ NaCl, and a pH of 8. No aggregation was observed at any areal density. Neither was aggregation observed for CaCl₂ concentrations up to 1.5 mol · L⁻¹ and times longer than 2 h.

where A is the Hamaker constant, R is the particle radius, D is the separation distance, and D is small compared to R . To a first approximation, $D \approx 0.2$ nm, $R = 195$ nm, and $A \approx 1 \times 10^{-20}$ J for PMMA acting across water.^[25] Since A is much smaller for PMMA interacting across DDMA, we can estimate the upper limit of E_{vdW} to be no more than $-200 k_B T$. The complications of calculating the attractive interactions along an interface and the uncertainty of A for PMMA across DDMA make the lower limit more difficult to evaluate. Nevertheless, the interaction between identical particles is always attractive regardless of the intervening medium. We can therefore suggest a lower limit of $-100 k_B T$, which is half the value for PMMA spheres in water.

Despite having such relatively large van der Waals attractions, the particles did not agglomerate when placed at a planar DDMA–water interface. Thermal fluctuations caused random dispersion in what is essentially a 2-D gas. The 390 nm PMMA particles, which were synthesized via a standard emulsion polymerization, possess no surface charge to our knowledge. We tested the possibility of surface charge by preparing additional planar samples (no vortexing) with various particle concentrations in the presence of 1.5 mol · L⁻¹ CaCl₂ buffer. Even after 2 h, we observed no noticeable agglomeration of the 390 nm PMMA particles for all particle densities, from very dilute concentrations up to 25% areal coverage. Note that while CaCl₂ will be depleted near the interface due to repulsion from image charges in the oil phase, the depletion zone will nonetheless be much smaller than the exposed hemisphere of PMMA.^[25]

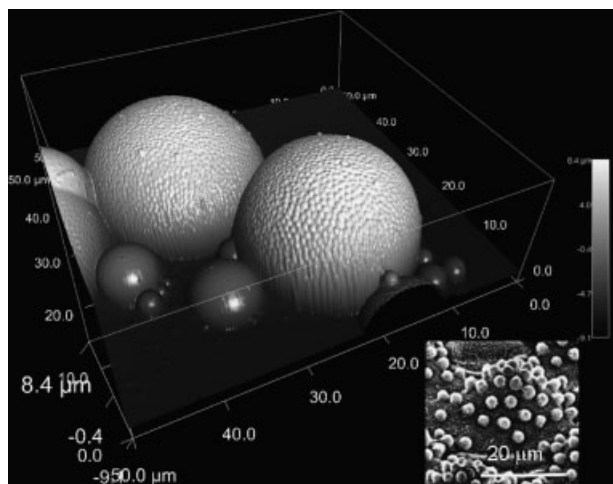


Figure 3. Comparison of an AFM image of a PMMA colloidosome assembly with that of the textured surface of a superhydrophobic *Hygoryza aristata* leaf (inset).^[4]

Also notable is the fact that the 390 nm PMMA particles are nearly centered at the interface. The average height of the exposed hemispheres was approximately 200 nm, indicating a three-phase contact angle of 90°. Such a result is surprising, for the PMMA particles disperse in DDMA but not water. Though these data also seem to suggest that some surface charge is present, the lower than expected contact angle with water may also result from excess polar groups on the surface, or unexpected contributions to the interfacial tension from the photoinitiator.

Young's law, for the case of a 90° contact angle, indicates that the particle–water interfacial tension (γ_{p-w}) and particle–oil interfacial tension (γ_{p-o}) are equal. The free energy change for placing a single particle at the interface, which is given by

$$\Delta E = -\frac{\pi R^2}{\gamma_{o-w}} [\gamma_{o-w} - (\gamma_{p-w} - \gamma_{p-o})]^2 \quad (2)$$

then reduces to $-\pi R^2 \gamma_{o-w}$, where γ_{o-w} is the oil–water interfacial tension. For $\gamma_{o-w} \approx 35 \text{ mJ} \cdot \text{m}^{-2}$, the free energy change is over a million times greater than the thermal energy at room temperature.^[25]

The three main forces in this system are therefore (1) hard-core repulsion, (2) van der Waals attraction, and (3) surface tension. Perhaps most interesting is the fact that different forces dominate at different length scales. At 1 μm , we see that the hard-core repulsion determines the local packing of the PMMA particles (Figure 2). Increasing in scale to 20 μm , we see that the interfacial tension pulls the PMMA particles together and sets the colloidosome diameter (Figure 3). Then at 50–100 μm the van der Waals attraction between the colloidosomes is now sufficiently large to overwhelm thermal fluctuations and draw them into small clusters (Figure 4). Finally, the morphology of the assemblies viewed beyond 100 μm is dictated by the hard-core repulsion of the colloidosomes insofar as the polydispersity causes inefficient packing (Figure 4).

A key concept is the primacy of interactions at the smallest length scale in setting the foundation for the assembly at all larger length scales. Control of the macroscopic structure and properties can, in some sense, be coded directly within the properties of the smallest building block. Taking the current example, the morphology in Figure 3 is almost completely controlled by the PMMA particles. Larger scale features such as colloidosome size, surface roughness, and colloidosome packing do not escape the influence of the particle diameter, surface energy, and concentration. While such interdependency may simplify the surface modification process, it may impose limitations when independent control of the structure at each generation of the hierarchy is desired. For the latter case, one must be able to isolate these different influences through the processing conditions. Fortunately, such control is afforded by the current assembly platform through the ability to rapidly crosslink nonequilibrium structures at discrete steps in the assembly process. Though it is beyond the scope of the current communication, studies are currently underway to resolve the effects of processing conditions on the resulting hierarchical morphologies.

We have demonstrated the use of a photocrosslinkable oil–water interface as a convenient platform for generating hierarchical topologies over multiple length scales. Due to the simplicity of the interaction potentials, the PMMA latex spheres serve as an excellent model system for understanding the controlling factors for organization at each length scale. We find that the balance between interfacial tension and hard-core repulsion dominates at small length scales, whereas van der Waals interactions become a factor at larger length scales.

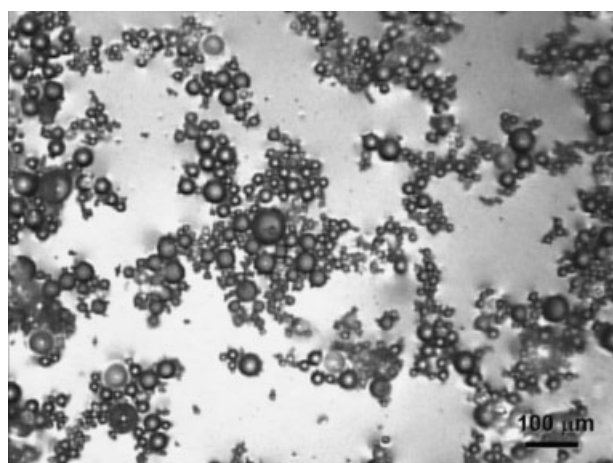


Figure 4. Light optical micrograph of colloidosome super-assemblies formed at the oil–water interface shown here after crosslinking and drying.

Acknowledgements: J. J. B. thanks the *National Research Council* for providing him with an NRC Fellowship. We acknowledge *Eric Amis* for support of the project, and the facilities provided by the *Polymers Division and Materials Science and Engineering Laboratory* for the project. We further thank *Jason Cleveland* and *David Beck* for help in obtaining AFM images. In addition, we thank *Ron Jones* and *Steve Hudson* for providing resources and for helpful discussions.

- [1] P. Ball, *Nature* **1999**, *400*, 507.
- [2] D. W. Bechert, M. Bruse, W. Hage, R. Meyer, *Naturwissenschaften* **2000**, *87*, 157.
- [3] P. Vukusic, J. R. Sambles, C. R. Lawrence, R. J. Wootton, *Proc. Bio. Sci., The Royal Society of London* **1999**, *266*, 1403.
- [4] C. Neinhuis, W. Barthlott, *Annal. Bot.* **1997**, *79*, 667.
- [5] D. Öner, T. J. McCarthy, *Langmuir* **2000**, *16*, 7777.
- [6] A. Lafuma, D. Quéré, *Nat. Mater.* **2003**, *2*, 457.
- [7] A. Nakajima, K. Hashimoto, T. Watanabe, *Monatsh. Chem.* **2001**, *132*, 31.
- [8] K. Autumn, Y. A. Liang, S. T. Hsieh, W. Zesch, W. P. Chan, T. W. Kenny, R. Fearing, R. J. Full, *Nature* **2000**, *405*, 681.
- [9] K. Autumn, M. Sitti, Y. A. Liang, A. M. Peattie, W. R. Hansen, S. Sponberg, T. W. Kenny, R. Fearing, J. N. Israelachvili, R. J. Full, *Proc. Natl. Acad. Sci.* **2002**, *99*, 12252.
- [10] A. K. Geim, S. V. Dubonos, I. V. Grigorieva, K. S. Novoselov, A. A. Zhukov, S. Y. Shapoval, *Nat. Mater.* **2003**, *2*, 461.
- [11] W. M. Gelbart, A. Ben-Shaul, *J. Phys. Chem.* **1996**, *100*, 13169.
- [12] J. T. Han, Y. Zheng, J. H. Cho, X. Xu, K. Cho, *J. Phys. Chem. B* **2005**, *109*, 20773.
- [13] T. Soeno, K. Inokuchi, S. Shiratori, *Appl. Surf. Sci.* **2004**, *237*, 543.
- [14] F. C. Cebeci, Z. Wu, L. Zhai, R. E. Cohen, M. F. Rubner, *Langmuir* **2006**, *22*, 2856.
- [15] A. S. Angelatos, K. Katagiri, F. Caruso, *Soft Matter* **2006**, *2*, 18.
- [16] O. D. Velev, A. M. Lenhoff, E. W. Kaler, *Science* **2000**, *287*, 2240.
- [17] G.-R. Yi, S.-J. Jeon, T. Thorsen, V. N. Manoharan, S. R. Quake, D. J. Pine, S.-M. Yang, *Synth. Mett.* **2003**, *139*, 803.
- [18] V. N. Manoharan, D. J. Pine, *MRS Bull.* **2004**, *29*, 91.
- [19] G.-R. Yi, V. N. Manoharan, E. Michel, M. T. Elsesser, S.-M. Yang, D. J. Pine, *Adv. Mater.* **2004**, *16*, 1204.
- [20] H. Duan, D. Wang, D. G. Kurth, H. Möhwald, *Angew. Chem. Int. Ed.* **2004**, *43*, 5639.
- [21] H. Duan, D. Wang, N. S. Sobal, M. Giersig, D. G. Kurth, H. Möhwald, *Nano. Lett.* **2005**, *5*, 949.
- [22] D. Wang, H. Duan, H. Möhwald, *Soft Matter* **2005**, *1*, 412.
- [23] Y. Lin, H. Skaff, T. Emrick, A. D. Dinsmoe, T. P. Russell, *Science* **2003**, *299*, 226.
- [24] J. T. Russell, Y. Lin, A. Böker, L. Su, P. Carl, H. Zettl, J. He, K. Sill, R. Tangirala, T. Emrick, K. Littrell, P. Thiyagarajan, D. Cookson, A. Fery, Q. Wang, T. P. Russell, *Angew. Chem. Int. Ed.* **2005**, *44*, 2420.
- [25] J. N. Israelachvili, "Intermolecular & Surface Forces", 2nd edition, Academic Press Inc., San Diego 1992, p. 315.